

## 2022 SNMMI Highlights Lecture: Oncology and Therapy, Part 2

Heiko Schöder

Memorial Sloan Kettering Cancer Center and Weill Cornell Medical College, New York, New York

The Highlights Lecture, presented at the closing session of each SNMMI Annual Meeting, was originated and presented for more than 30 y by Henry N. Wagner, Jr., MD. Beginning in 2010, the duties of summarizing selected significant presentations at the meeting were divided annually among 4 distinguished nuclear and molecular medicine subject matter experts. The 2022 Highlights Lectures were delivered on June 14 at the SNMMI Annual Meeting in Vancouver, Canada. This month we feature the second part of the lecture by Heiko Schöder, MD, MBA, Chief of the Molecular Imaging and Therapy Service in the Department of Radiology at Memorial Sloan Kettering Cancer Center and professor of radiology at Weill Cornell Medical College (both in New York, NY), who spoke on oncology and therapy topics at the meeting. Note that in the following presentation summary, numerals in brackets represent abstract numbers as published in *The Journal of Nuclear Medicine* (2022;63[suppl 2]).

**Key Words:** oncology; radionuclide therapy; theranostics

**J Nucl Med 2023; 64:2–7**

DOI: 10.2967/jnumed.122.265202

In the first part of this lecture, I addressed notable trends seen in presentations at this year's SNMMI Annual Meeting and reviewed clinical diagnostic areas of current interest. Here we look briefly at clinical radionuclide therapy and experimental studies, with a few concluding thoughts on oncology and therapy in our field.

### CLINICAL RADIONUCLIDE THERAPY

It is important to carefully assess the criteria for inclusion in our studies and the implications these have across the spectrum of disease severity and manifestations, including for those who do not meet treatment criteria. We are all familiar with the promising results of the VISION trial and its various follow-ups evaluating  $^{68}\text{Ga}$ -prostate-specific membrane antigen (PSMA)-11 imaging and  $^{177}\text{Lu}$ -PSMA-617 treatment in men with PSMA-expressing metastatic castration-resistant prostate cancer (mCRPC). The inclusion criteria for the trial were  $\geq 1$  PSMA-positive metastatic lesion and no PSMA-negative metastatic lesions. These criteria produced a screen failure rate of 12.6%. PSMA positivity is a prerequisite criterion for most PSMA-targeted radioligand therapies; however, the definition of this positivity differs among studies. Hotta et al. from the University of California Los Angeles looked more closely at groups that would have been excluded from the VISION trial in

their report on “Outcome of patients with PSMA PET/CT screen failure by VISION criteria and treated with  $^{177}\text{Lu}$ -PSMA therapy: A multicenter retrospective analysis” [3039]. They asked whether the VISION PET criteria are appropriate to identify patients who will not benefit from  $^{177}\text{Lu}$ -PSMA treatment. The retrospective study included 301 patients who had undergone  $^{177}\text{Lu}$ -PSMA-617 treatment, of whom 29 (9.7%) would have been screen failures (21 with PSMA-negative lesions and 8 with low PSMA expression) in the VISION trial. Outcome measures included response and survival data. When the authors compared outcomes over a median 1-y follow-up, they found that patients who would have been screen failures in the VISION trial had worse prostate-specific antigen (PSA) response rates and shorter median overall survival (OS). Screen failure patients with PSMA-negative lesions ( $n = 21$ ) tended to have worse responses than those with low PSMA expression ( $n = 8$ ). The conclusion is that patients who do not show sufficient PSMA uptake or have lesions that do not qualify based on well-defined criteria are likely to see inferior outcomes. The authors provided a cautionary note that “not characterizing target expression before PSMA-targeted treatment appears now nonethical, as a predictive whole-body imaging biomarker for response to PSMA-targeted therapies is available.”

In this Highlights lecture last year, I was able to only briefly address therapy with  $\alpha$ -emitters, which are receiving more attention and are the focus of multiple efforts to provide greater availability. Bal et al. from the All India Institute of Medical Sciences (New Delhi) reported on a “Long-term outcome study on  $^{225}\text{Ac}$ -PSMA-617 targeted  $\alpha$ -therapy in mCRPC: A prospective, single-institutional study” [2546]. The study included 50 patients whose disease was refractory to other therapy options (including 31 patients refractory to previous  $^{177}\text{Lu}$ -PSMA-617 treatment). Molecular tumor evaluation after  $\alpha$ -therapy showed complete response in 3 (6%), partial response in 16 (32%), stable disease in 11 (22%), and progressive disease in 20 (40%) patients, for an overall disease control rate of 60% according to molecular response. Thirty-one patients (62%) died during the treatment period, with an estimated median OS of 14 mo and 12- and 24-mo survival probabilities of 57.6% and 34%, respectively. Estimated median progression-free survival was 11 mo with a 12-mo progression-free survival probability of 43%. Treatment-related toxicities were minimal. Figure 1 shows very impressive results in a heavily pretreated patient.

The same group also reported on “A phase II clinical study on  $^{225}\text{Ac}$ -DOTATATE therapy in advanced-stage gastroenteropancreatic neuroendocrine tumor (GEP NET) patients” [2208]. This phase 2



Heiko Schöder, MD, MBA

Received Nov. 15, 2022; revision accepted Nov. 15, 2022.

For correspondence or reprints, contact Heiko Schöder (schoderh@mskcc.org).  
COPYRIGHT © 2023 by the Society of Nuclear Medicine and Molecular Imaging.

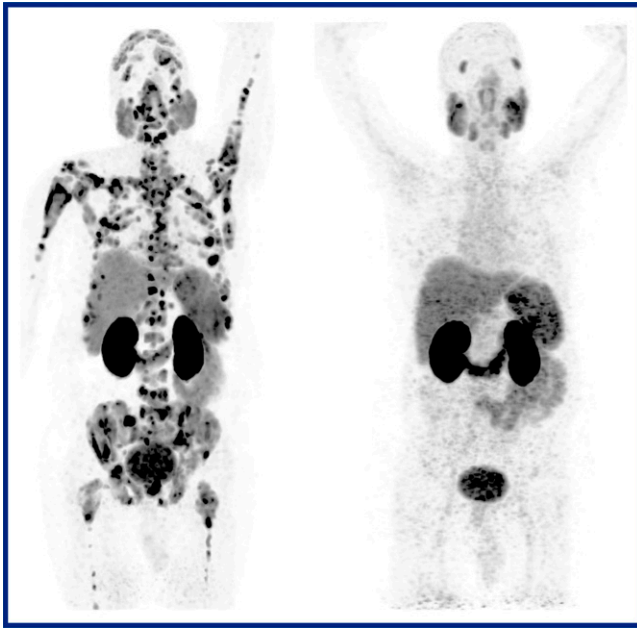


**FIGURE 1.** Long-term outcomes in  $^{225}\text{Ac}$ -PSMA-617 targeted  $\alpha$ -therapy in metastatic castration-resistant prostate cancer. Example shows results after 5 cycles of  $^{225}\text{Ac}$ -PSMA-617 in a heavily pretreated patient who had progressed under standard treatment and with disease refractory to  $^{177}\text{Lu}$ -PSMA-617.

study followed up on earlier work and included 83 patients (49 men, 34 women), 56 of whom had undergone prior  $^{177}\text{Lu}$ -DOTATATE treatment and 27 of whom were  $^{177}\text{Lu}$ -DOTATATE naïve. Systemic  $^{225}\text{Ac}$ -DOTATATE (100–120 kBq/kg bodyweight) along with a renal protection protocol were administered intravenously at 8-weekly intervals (median, 4 cycles/patient; range, 1–10 cycles). Over a median follow-up of 18 mo (range, 2–34 mo), 24 (29%) patients died, with 12- and 24-mo OS of 85.3% and 67.6%, respectively. Seventy-four of the patients underwent radiographic assessment over a median follow-up of 18 mo. Of these, (2.7%) had a complete response; 32 (43.2%) had a partial response, 25 (34%) had stable disease, and 15 (20%) had progressive disease (Fig. 2). A higher percentage of progressive disease was observed in prior  $^{177}\text{Lu}$ -DOTATATE failure patients (34%) than in  $^{177}\text{Lu}$ -DOTATATE-naïve patients (11%). Side effects were deemed acceptable. These are encouraging data that clearly justify further exploration of  $^{225}\text{Ac}$ -DOTATATE therapies.

As I noted earlier in this lecture, a growing challenge in our new therapies is to track multiple lesions over time, and artificial intelligence (AI) is providing novel strategies. Perk et al. from AIQ Solutions (Madison, WI) and the University of Wisconsin Madison reported on “Automated evaluation of disease on  $^{68}\text{Ga}$ -DOTATATE PET/CT images for long-term lesion tracking on  $^{177}\text{Lu}$ -DOTATATE therapy” [2580]. The retrospective study included sequential  $^{68}\text{Ga}$ -DOTATATE PET/CT images from 25 patients with GEP NETs during  $^{177}\text{Lu}$ -DOTATATE therapy. Total SUV was automatically tracked across scans, and response was classified into 5 categories based on change in SUV between serial scans. Patients were determined to have

heterogeneous response if they had both favorably responding (complete or partial response) and unfavorably responding lesions (progressive disease or new lesions). On the first follow-up scan, 24 of the 25 patients showed heterogeneous response. Across all patients in the course of the study, 523 lesions completely resolved after the start of treatment (range, 1–115/patient), and 756 new lesions were detected (range, 0–185/patient). In the subset of 12 patients who had  $\geq 3$  scans, 28 (8%) of 378 completely resolved lesions returned on subsequent imaging, whereas 159 (45%) of 355 new lesions resolved on subsequent scans. At final follow-up scan, patients had a median of 23% (range, 7%–61%) progressive and 63% (range, 21%–82%) responding lesions. Figure 3 shows examples of the automated response assessment classification of heterogeneous changes. Documentation of complex changes using automated response assessment shows promise for monitoring both the heterogeneity of tumor response and evolving tumor burden during radionuclide therapies, with important implications for more individualized management. This will enable us to track each individual lesion over time rather than make a summary statement that the patient as a whole is responding, which fails to address the entire biology of the underlying disease and response.

Dosimetry is increasingly important for treatment planning in radionuclide therapies. Jackson et al. from the Peter MacCallum Cancer Centre (Melbourne, Australia) and Precision Molecular Imaging and Theranostics (Melbourne, Australia) reported on “Real-world lesion and renal dosimetry for peptide receptor radionuclide therapy (PRRT)” [2110]. The purpose of the study was to assess the feasibility of comprehensive lesion and organ posttherapy SPECT/CT dosimetry in routine follow-up of  $^{177}\text{Lu}$ -DOTATATE PRRT and evaluate the impact of lesional radiation dose on change in target volume over multiple cycles. The study included 97 patients with a range of neuroendocrine neoplasias in whom dosimetry for kidneys and index lesions was assessed on quantitative SPECT/CT imaging 24 h after each PRRT cycle. Dose values were comparable for the different grades of disease, but, remarkably, dose to the index lesion decreased by 25.5%, 38.7%, and 45.3% at cycles 2, 3, and 4. Renal doses per GBq increased by  $4\% \pm 19\%$ ,  $13\% \pm 24\%$ , and  $12\% \pm 24\%$  at corresponding cycles. The conclusion was that many patients treated with the current standard activity are actually undertreated and could receive a higher initial activity, with subsequent administered activities adjusted “on the fly” using dosimetry to maximize tumor dose and decrease renal

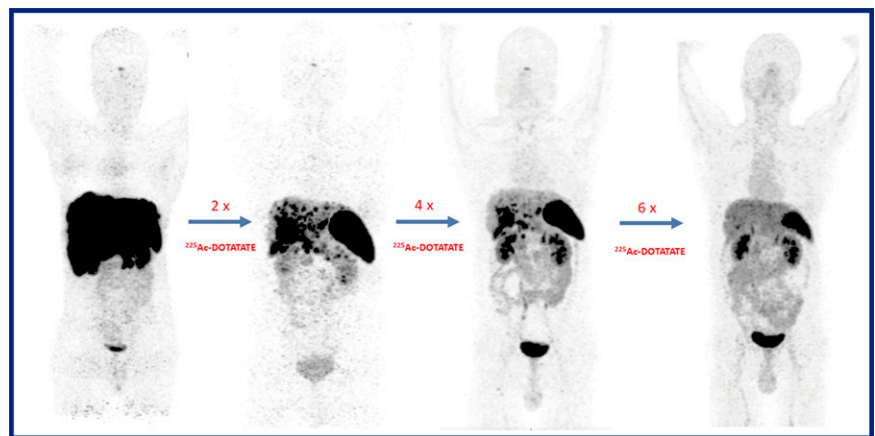


**FIGURE 2.**  $^{225}\text{Ac}$ -DOTATATE therapy in advanced-stage gastroenteropancreatic neuroendocrine tumors. Example maximum-intensity projection  $^{68}\text{Ga}$ -DOTANOC PET images from a patient at (left to right) baseline and after 2, 4, and 6 cycles of  $^{225}\text{Ac}$ -DOTATATE.

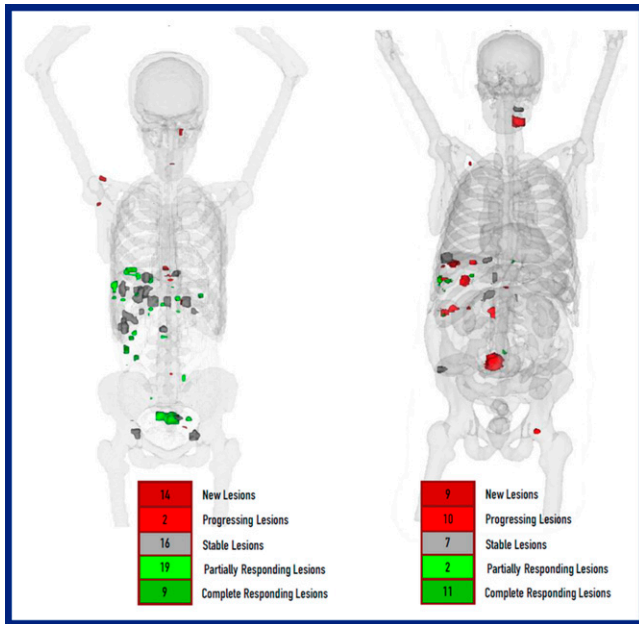


**FIGURE 3.** Automated evaluation of gastroenteropancreatic neuroendocrine tumor status on  $^{68}\text{Ga}$ -DOTATATE PET/CT for long-term lesion tracking in  $^{177}\text{Lu}$ -DOTATATE therapy. Total SUV was automatically tracked across scans, with responses classified into 5 categories based on change between serial scans. Documentation of complex changes using automated response assessment shows promise for monitoring both heterogeneity of tumor response and evolving tumor burden during radionuclide therapies, with implications for more individualized management.

dose. The authors concluded that “in most cases, this would allow a significant increase in prescribed activity with potential improvement in treatment efficacy and preserved safety.”

Kappadath et al. from the University of Texas MD Anderson Cancer Center (Houston) reported on “Radioembolization for hepatocellular cancer (HCC) patients with personalized  $^{90}\text{Y}$  dosimetry for curative intent (RAPY $^{90}\text{D}$ ): An interim analysis” [2375]. This trial looks at  $^{90}\text{Y}$ -glass radioembolization using patient-specific voxel-dosimetry treatment planning with  $^{99\text{m}}\text{Tc}$ -macroaggregated albumin ( $^{99\text{m}}\text{Tc}$ -MAA) SPECT/CT. The primary goal was a localized objective response rate (ORR) of  $> 75\%$  at 6-mo follow-up with a targeted mean tumor dose of 200 Gy to all tumors  $\geq 3$  cm. They also studied concordance between planned and delivered doses. The researchers were about halfway through enrollment at the time of the SNMMI Annual Meeting. In 21 patients, they saw ORRs of 56% and 96% at 3 and 6 mo, with corresponding complete response rates of 33% and 56%, thus meeting their primary objective. I want to point out that the study included patients with large lesions (median diameter, 4.6 cm), much larger than those in the widely cited LEGACY study (median diameter, 2.7 cm) (Fig. 4). In addition, they found high correlations between the predicted dose from  $^{99\text{m}}\text{Tc}$ -MAA SPECT/CT treatment planning and the actual dose received. Their finding that radioembolization treatment plans targeting high dose to tumors ( $\geq 200$  Gy) and minimizing dose to normal liver had so far resulted in 100% tumor response rates with no treatment-related toxicities is encouraging, and we look forward to publication of the final study results.

#### EXPERIMENTAL STUDIES

Many promising research studies were presented at this year’s meeting. I will limit these highlights to only a small selection.

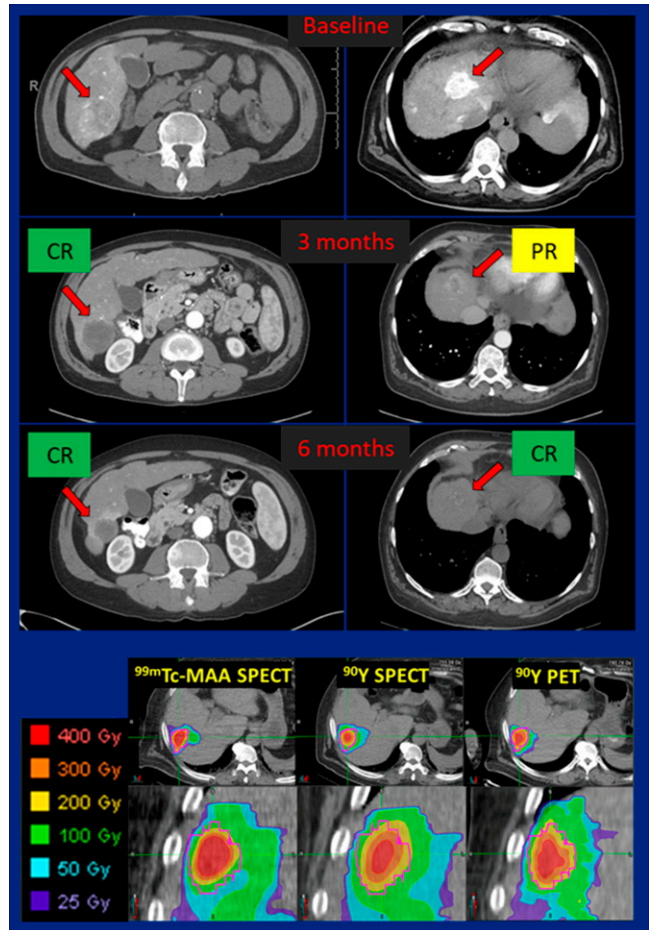


**FIGURE 4.** Radioembolization for hepatocellular cancer with personalized  $^{90}\text{Y}$  dosimetry for curative intent (RAPY $^{90}\text{D}$ ). Patient-specific voxel-dosimetry treatment planning with  $^{99\text{m}}\text{Tc}$ -macroaggregated albumin ( $^{99\text{m}}\text{Tc}$ -MAA) SPECT/CT. Top block: Example imaging from 2 patients at baseline (top row), 3 mo (middle row), and 6 mo (bottom row) after radioembolization. CR = complete response; PR = partial response. Bottom block: Absorbed dose maps (left to right, with  $^{99\text{m}}\text{Tc}$ -MAA SPECT,  $^{90}\text{Y}$  SPECT, and  $^{90}\text{Y}$  PET) in a patient treated with 0.710 GBq  $^{90}\text{Y}$  to deliver a mean dose of 316 Gy, with a complete response at 3 and 6 mo. High correlations were noted between predicted dose from  $^{99\text{m}}\text{Tc}$ -MAA SPECT/CT treatment planning and actual dose received.

Lee et al. from the University of Pennsylvania (Philadelphia) reported on “Monitoring therapeutic response to fibroblast-activation protein (FAP) chimeric antigen receptor (CAR) T-cells using  $^{18}\text{F}$ -AIF-FAP inhibitor (FAPI)-74 PET” [2499]. After the SNMMI Meeting, this study was published in *Clinical Cancer Research* (2022; Aug 16 ahead of print). The authors characterized the selectivity of the radiotracer in in vitro and xenograft studies and then conducted a series of investigations with tumor xenograft models in mouse groups treated with FAP CAR T-cells and with nontransduced cells. Figure 5 shows intense uptake and a 2- (SUV $_{\text{mean}}$ ) to 3-fold (SUV $_{\text{max}}$ ) reduction in tumor-to-muscle ratio from baseline for the FAP CAR T-cell-treated group compared with continued tumor growth in the nontransduced cell-treated group. The authors concluded that “this noninvasive imaging approach to interrogate the tumor microenvironment is the first pairing of a companion diagnostic for solid tumor CAR T-cell therapy and has the potential to serve as a predictive and pharmacodynamic response biomarker geared specifically for FAP CAR

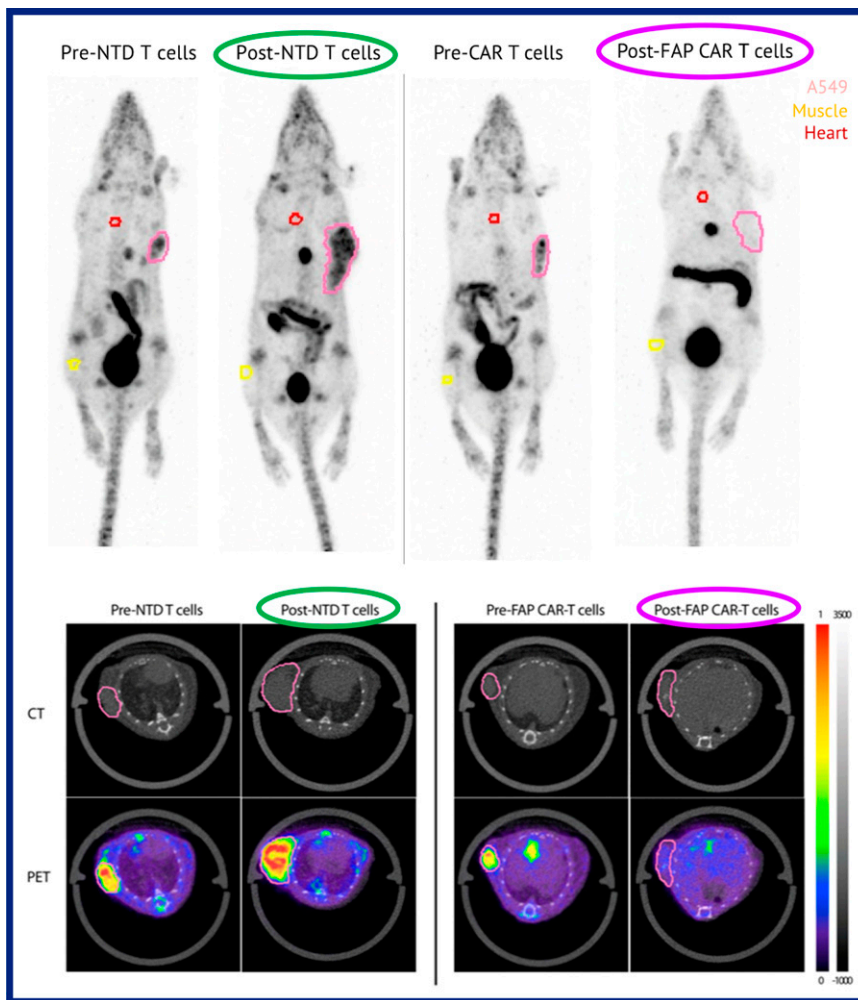


**FIGURE 5.** Monitoring therapeutic response to fibroblast-activation protein (FAP) chimeric antigen receptor (CAR) T-cells using  $^{18}\text{F}$ -AIF-FAP inhibitor (FAPi)-74 PET. Top block: Mice at baseline and after treatment with nontransduced CAR T-cells (left) and FAP CAR T-cells (right), showing intense uptake and a 2- to 3-fold reduction in tumor-to-muscle ratio from baseline. Bottom block: Corresponding PET/CT images.

T cell therapy.” Note that FAP CAR T-cell treatment shows a decrease in but not complete elimination of tumor, leading some researchers to speculate that FAP-directed CAR T-cells may address the stroma but not necessarily kill the tumor. This may be of special relevance in advancing FAP-directed radiotheranostics.

Immunotherapy continues to be the focus of much research in the nuclear medicine community. Predicting which patients are likely to benefit from immunotherapies is currently quite challenging with standard-of-care cancer imaging techniques. Evans et al. from the University of California, San Francisco, reported on “Getting a GRIP on antitumor immunity with granzyme-targeted PET” [2497]. The authors hypothesized that because immune cells (e.g., cytotoxic T-cells, natural killer cells) secrete serine proteases called granzymes to impart apoptosis in cancer cells, an imaging tool capable of detecting biochemically active granzyme B could be a useful biomarker to distinguish immunoresponsive from immunoresistant tumors in vivo. In their presentation, they outlined an elegant approach using a restricted-interaction peptide, which they call GRIP B. GRIP B was confirmed in vitro to be a substrate for granzyme B and was labeled with  $^{64}\text{Cu}$  for initial

in vivo studies. Imaging in animals treated 3 times with combined immunotherapy and then injected with  $^{64}\text{Cu}$ -GRIP B showed that the signal increased over time. Digital autoradiography in the same mice showed that the tracer indeed localizes as expected, with an inverse relationship between the intensity of uptake and growth inhibition. The authors concluded that  $^{64}\text{Cu}$ -GRIP B provides a holistic view of secreted granzyme B biochemistry in vivo and that posttreatment changes in tumor uptake approximate responses to checkpoint inhibitors. They are currently preparing for first-in-humans studies and investigating potential applications of  $^{64}\text{Cu}$ -GRIP B in other immunomodulatory therapies.

In another interesting study from the same lab, Chopra et al. from the University of California, San Francisco, reported that the “CUB domain-containing protein 1 (CDCP1) is a target for radioligand therapy in multiple bladder cancer subtypes, including Nectin-4 and TROP2 null disease” [2563]. CDCP1 is a cell surface protein highly overexpressed in many cancer types, with low expression in normal tissues. Its potential for treatment in pancreatic and prostate cancer has been explored. These authors wanted to determine whether bladder cancer overexpresses CDCP1, and whether CDCP1 can be targeted for treatment with radiolabeled antibodies. This research is welcome, because relatively little work has been done with radioligand therapy in bladder cancer, particularly in aggressive forms. In in vitro and preclinical studies, the researchers found that CDCP1 mRNA and protein levels were expressed in multiple subtypes of bladder cancer, with a tendency toward higher expression in the basal subtype of bladder cancer. Using PET with  $^{89}\text{Zr}$ -4A06

(a monoclonal antibody targeting a domain of CDCP1), CDCP1 was detectable in 6 human bladder cancer tumors. An antitumor assessment in mice showed that fractionated doses of  $^{177}\text{Lu}$ -4A06 significantly inhibited the growth of tumor xenografts and improved OS. In a representative cohort, 4 of 8 mice experienced complete responses and no tumor regrowth was observed over 3 mo of monitoring (Fig. 6). Of note, CDCP1 expression did not entirely overlap with Nectin-4 or TROP2, suggesting that CDCP1-directed strategies may have a role in bladder cancer treatment distinct from current standards of care.

Feng et al. from Duke University (Durham, NC) reported on “Therapeutic efficacy of an  $^{211}\text{At}$ -labeled anti-HER2 single-domain antibody fragment (sdAb) in mice: Comparison with its  $^{131}\text{I}$ -labeled analog” [2565], which brings us back to  $\alpha$ -emitter therapy, where we have to ask what designs and radiolabeling approaches are optimal. Astatine is an  $\alpha$ -emitter with a 7.2-h half-life. In a series of investigations they showed high in vivo stability, good radiochemical yield, rapid normal tissue clearance, and high binding to HER2-expressing BT474 human breast carcinoma xenografts. When they applied their  $^{211}\text{At}$ -iso-SAGMB-VHH\_1028 agent in mice, a single

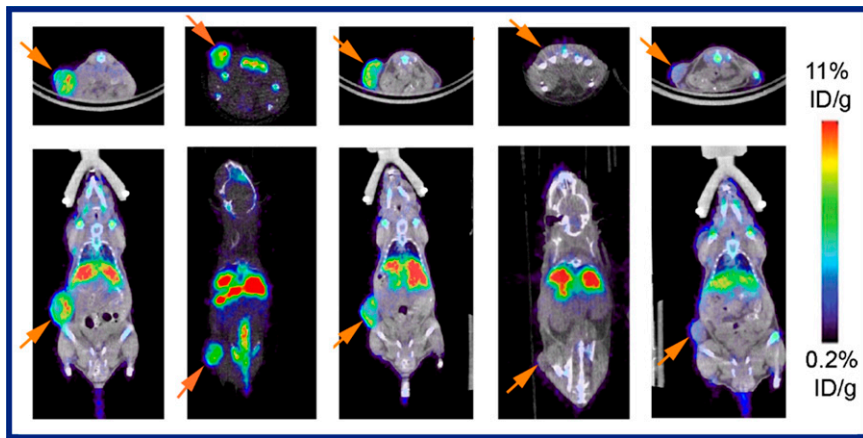


**FIGURE 6.** CUB domain-containing protein 1 (CDCP1) as a target for radioligand therapy in bladder cancer.  $^{89}\text{Zr}$ -4A06 PET detected CDCP1 in 6 human bladder cancer tumors (left to right: UMUC3, T24, HT1376, UMUC9, and 5637) at 72 h postinjection. Fractionated doses of  $^{177}\text{Lu}$ -4A06 significantly inhibited growth of tumor xenografts and improved overall survival, suggesting the potential for CDCP1-directed theranostic strategies.

dose increased median survival by > 400% with no observable signs of normal tissue toxicity and complete absence of tumor observed in the majority of animals treated at median and high doses. This compared favorably with results from 3 treatments with  $^{131}\text{I}$ -labeled antibody.

Identifying the right chelator is important for the stability of a radiotherapeutic compound. Abou et al. from Washington University in St. Louis/Washington University School of Medicine (MO) and the Université d'Avignon et des Pays du Vaucluse (France), Institut de Chimie de Strasbourg IC-UNISTRA (France), Institut de Chimie Moléculaire de l'Université de Bourgogne (Dijon, France), Lumiphore Inc. (Berkeley, CA), and the Mallinckrodt Institute of Radiology (St. Louis, MO) reported on "Comparing 4 chelators of  $^{227}\text{Th}$  and antibody conjugates for  $\alpha$ -emitting radioimmunotherapy" [2568]. They detailed comparisons in ease of labeling, in vivo stability, conservation of immunoreactivity, and tumor targeting and concluded that their  $^{227}\text{Th}$ -ThL804 immune complex showed the best characteristics as a chelator in both lymphoma and HER2 cancer model studies. In a HER2-expressing colon cancer mouse model,  $^{227}\text{Th}$ -ThL804-trastuzumab treatment led to positive preliminary results. The L804 agent can also be labeled with  $^{89}\text{Zr}$  for imaging, supporting development of  $^{227}\text{Th}$  theranostic applications.

Wichmann et al. from the Olivia Newton-John Cancer Research Institute, the University of Melbourne, and Austin Health/Austin Hospital (all in Melbourne, Australia) reported on "Conjugation and radiolabeling of  $^{225}\text{Ac}$ -macropa-tzPEG3Sq-ch806, a tumor-specific anti-epidermal growth factor receptor (anti-EGFR) antibody, and preclinical evaluation in a murine glioma model" [2569].

https://doi.org/10.1195/journal.1195.2022.01.001

development of an agent for radioimmunotherapy with  $^{225}\text{Ac}$  complexed to ch806, the chimeric form of mAb806, a monoclonal antibody targeting EGFR. They detailed several experiments proving high purity and radiochemical yield, as well as exquisite tumor targeting in vivo. Biodistribution and uptake studies in mice were promising, and in vivo therapy studies in a mouse glioma model showed marked tumor responses and prolonged survival in an  $^{225}\text{Ac}$ -ch806-treated cohort compared with controls. This approach, with fast and efficient labeling of antibodies resulting in radioimmunoconjugates with exceptional stability, addresses current challenges of  $^{225}\text{Ac}$  complexation and points to expanded applications in multiple diseases

Liposomal drugs have been in use for some time, and we are all familiar with pegylated doxorubicin. Hwang et al. from Seoul

National University (Republic of Korea) reported on "Theranostic gemcitabine-loaded collagenase conjugated liposome (GCL)" [4054]. These researchers used the enhanced-permeability-and-retention effect to localize the conjugate in the tumor, with collagenase on the surface of the liposome for degradation of the extracellular matrix enabling "smart drug delivery." This may be of particular interest in pancreatic cancer, where dense stroma prevents penetration of the drug into the tumor. The GCL agent showed potent collagenase activity, passive tumor-targeting ability, and enhanced tumor penetration.  $^{68}\text{Ga}$ -labeling for PET imaging in a CT-26 tumor-bearing mouse model

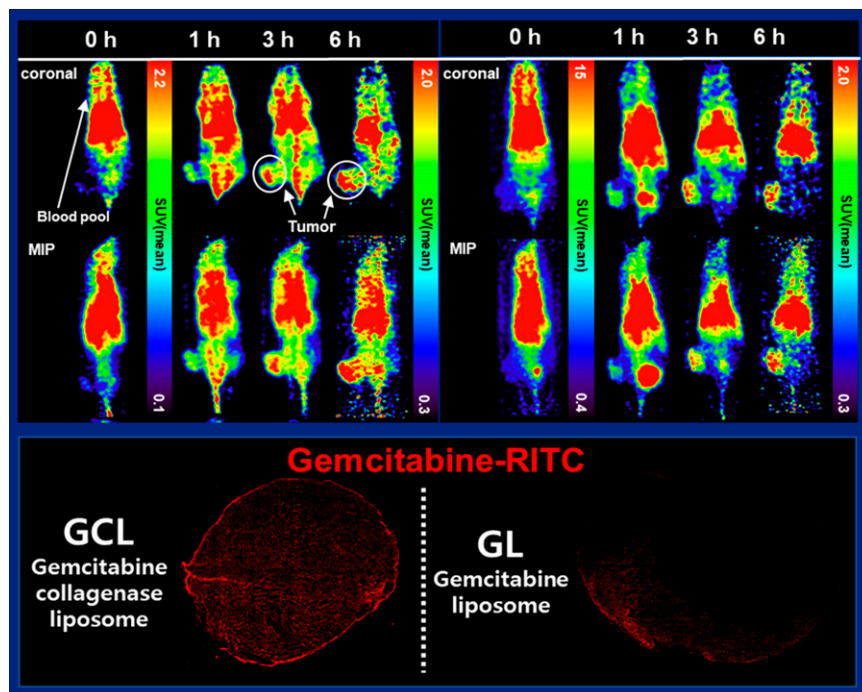


**FIGURE 7.** Theranostic gemcitabine-loaded collagenase conjugated liposome (GCL) for solid tumor targeting. Top: GCL (left) and unmodified PEGylated liposome (right) were labeled with  $^{68}\text{Ga}$ , injected intravenously in a CT-26 tumor-bearing mouse model, and imaged with PET, showing similar prominent tumor uptake. Bottom: Collagenase in the GCL agent (left) enhanced tumor penetration compared with a gemcitabine-only liposome.

confirmed tumor targeting (Fig. 7), indicating potential as part of a theranostic pair for solid tumors such as pancreatic cancer.

I began the discussion of new experimental studies with FAP inhibitors and ended with collagen, stroma, and fibroblasts. I want to just add a small word of caution, however. A recent review article by Pich et al. in *Cancer Cell* (2022;40[5]:458–478) noted that the early promise of precision-based and personalized treatment has not been fully realized. Many factors, including epigenetic changes, resistance mechanisms, and others, confound our efforts. Cancer-associated fibroblasts, for example, can have many roles, including interactions with the immune environment. The stromal matrix, usually thought to inhibit chemotherapy in pancreatic cancer, has in fact been shown in some studies to inhibit cancer progression. In other words, regarding radiolabeled FAPI or any other novel type of agent as a “magic bullet” may be naïve. Many mechanisms interfere with our sometimes simplistic hopes for how cancer can be treated. A greater understanding and much more investigation of the tumor microenvironment, different fibroblast entities, and stroma are needed.

### **CLOSING THOUGHTS**

The more tracers and applications we develop, the more questions we have. For PSMA, for example, we have to ask how many

more probes are actually needed. We must settle on some subset of the possible number, but more important is the need to define the roles of PSMA in specific clinical settings, including at different states of disease. We need to design probes for the more advanced and dedifferentiated prostate cancers that will become of greater interest as we are more and more successful at treating earlier states of disease that still express PSMA. For FAPI, as I noted last year, we still need data from large prospective trials and clinical experience, both in diagnosis and therapy. I was encouraged to see that some of this work is beginning.

Major tasks for the future are numerous. Clinical translation of new probes to the clinic is crucial. This is difficult, time consuming, and expensive but necessary to make a difference in patients’ lives. We are making progress in defining the role of  $\alpha$ -emitters and  $\alpha$ -labeled radiopharmaceuticals, but we must provide evidence-supported data defining their role and appropriate applications. We need more data and more focus on dosimetry in radionuclide therapy, using this to refine and individualize our treatments. Finally, we must acknowledge and address together a host of clinical (e.g., treatment resistance, combination therapies) and professional (e.g., workforce stability, reimbursement, patient access) challenges.